



Selection of single-source multifragmentation events for collisions of $^{155}\text{Gd}+^{238}\text{U}$ at 36 MeV/u studied with INDRA

J.D. Frankland, Ch.O. Bacri, B. Borderie, R. Bougault, J.F. Lecolley, M.F. Rivet, M. Squalli, M. Assenard, G. Auger, J. Benlliure, et al.

► To cite this version:

J.D. Frankland, Ch.O. Bacri, B. Borderie, R. Bougault, J.F. Lecolley, et al.. Selection of single-source multifragmentation events for collisions of $^{155}\text{Gd}+^{238}\text{U}$ at 36 MeV/u studied with INDRA. International Winter Meeting on Nuclear Physics 35, Feb 1997, Bormio, Italy. pp.323-342. in2p3-00023110

HAL Id: in2p3-00023110

<https://hal.in2p3.fr/in2p3-00023110>

Submitted on 29 Jun 1999

HAL is a multi-disciplinary open access archive for the deposit and dissemination of scientific research documents, whether they are published or not. The documents may come from teaching and research institutions in France or abroad, or from public or private research centers.

L'archive ouverte pluridisciplinaire **HAL**, est destinée au dépôt et à la diffusion de documents scientifiques de niveau recherche, publiés ou non, émanant des établissements d'enseignement et de recherche français ou étrangers, des laboratoires publics ou privés.

SCAN-9704077



CERN LIBRARIES, GENEVA

504745

*Contribution to the XXXV Int. Winter Meeting on Nuclear Physics,
Bormio (Italy), February 3-7, 1997*
J.D. FRANKLAND and the INDRA collaboration

**SELECTION OF SINGLE-SOURCE MULTI-
FRAGMENTATION EVENTS FOR COLLISIONS
OF $^{155}\text{Gd}+^{238}\text{U}$ AT 36 MeV/u STUDIED WITH INDRA**

| | |
|----------------|-----------------------|
| IPNO-DRE-97-10 | CEA/DAPNIA/SPhN 97-15 |
| GANIL P 97 07 | LPCC 97-06 |
| LYCEN/9709 | SUBATECH-97-06 |

Selection of single-source multifragmentation events for collisions of $^{155}\text{Gd}+^{238}\text{U}$ at 36MeV/u studied with INDRA

J.D. Frankland¹

and the INDRA collaboration

Ch.O. Bacri¹, B. Bortolotto¹, R. Bougault³, J.F. Leclercq³, M.F. Rivet¹, M. Squall¹, M. Assenard⁶, G. Auger², J. Benlliure², E. Bisquer⁴, F. Bouchet³, R. Brou³, P. Buchet⁵, J.L. Charvet⁵, A. Chbibi², J. Colin³, D. Cussol³, R. Dayras⁵, E. De Filippo⁵, A. Demeyer⁴, D. Doré¹, D. Durand³, P. Eudes⁶, E. Galichet⁴, E. Genouin-Duhame³, E. Gerlic⁴, M. Germain⁶, D. Gouriou⁶, D. Guinet⁴, P. Lautesse⁴, J.L. Laville⁶, A. Le Fèvre², T. Lefort³, R. Legrain⁵, O. Lopez³, M. Louvel³, N. Marie², V. Méhervier⁶, L. Nalpas⁵, A.D. Nguyen³, M. Parlog⁷, J. Pétér³, E. Plagnol¹, A. Rahmani⁶, T. Reposeur⁶, E. Rosato⁸, R. Roy⁹, F. Saint-Laurent², S. Salou², J.C. Steckmeyer³, M. Stern⁴, G. Tabacaru⁷, B. Tannai³, O. Tirié³, L. Tassan-Got¹, E. Vient³, C. Volant⁵, J.P. Wieleczko²

¹ Institut de Physique Nucléaire, IN2P3-CNRS, 91106 Orsay Cedex, France.

² GANIL, CEA, IN2P3-CNRS, B.P. 5027, 14021 Caen Cedex, France.

³ LPC, IN2P3-CNRS, ISMRA et Université, 14050 Caen Cedex, France.

⁴ IPN Lyon, IN2P3-CNRS et Université, 69622 Villeurbanne Cedex, France.

⁵ CEA, DAPNIA/SPN, CEN Saclay, 91191 Gif sur Yvette Cedex, France.

⁶ SUBATECH, IN2P3-CNRS et Université, 44072 Nantes Cedex 03, France.

⁷ Institute of Physics and Nuclear Engineering, IFN, P.O. Box MG6,

Bucharest, Romania.

⁸ Dipartimento di Scienze, Univ. di Napoli, 80125 Napoli, Italy.

⁹ Laboratoire de Physique Nucléaire, Département de Physique, Université Laval, Québec G1K7P4, Canada.

Abstract

Commonly-used approaches to selecting so-called ‘single-source’ events in GANIL energy heavy-ion collisions are discussed and compared, using as an example the system Gd+U 36MeV/u studied with the INDRA 4 π -detector. Of the methods considered, based on global analyses of multiplicity, energy, and momenta, the so-called ‘Wilczyński diagram’ technique is shown to have the best performance in terms of the statistics of the selected sample of events and pollution by other reaction mechanisms. The cross-section of single-source events for the system Gd+U is found to be ~ 41 mb.

1 Introduction and Motivations

‘Single-source’ events in heavy-ion collisions at 20 - 100MeV/u, in which the near-totality of the available mass and excitation energy of the colliding system are comprised in one single multifragmenting source, have been well isolated and characterised for several heavy systems [1][2][3][4][5] using the so-called ‘Wilczyński diagram’ technique, presented in detail in this contribution. Such events have several interesting and unique features :

- the available excitation energy for the single source is the maximum possible
- the fragmenting source is the largest piece of excited nuclear matter that may be formed for collisions of a given system and, for heavy systems, beyond the size of the largest nuclei known to occur in nature ($A_{\text{max}} \geq 250$). The large size of the source implies that, if instabilities occur, volume (i.e. spinodal) rather than surface (e.g. Rayleigh) effects are likely to dominate, while any collective behaviour (e.g. radial flow due to initial compression of the matter) if present is likely to be significant
- in the same way as the mass of the single source may be beyond those normally encountered in nuclei, so may be its charge-to-mass ratio, which suggests potential Coulomb instability effects[6][7]

Overall the study of single-source events, especially for heavy systems, presents an opportunity to quantify the relative importance of these various effects in the multifragmentation process. However experimental evidence for many systems at GANIL bombarding energies shows heavy-ion collisions to be dominated by dissipative reactions which are binary in character (two excited fragmenting sources in the exit channel)[8][9][10][11], and that single-source events, when they have been properly isolated, account for no more than $\sim 1\%$ of σ_R [2][4]. It is therefore crucial to the analysis to study the performance of available selection methods for the system in question, and to choose the one which minimises any eventual pollution by the dominant binary reactions.

Collisions of Gd+U at 36MeV/u have been studied at the GANIL facility using the 4 π detector INDRA[12], whose main characteristics are : detection and identification of charged particles with unit charge resolution from $Z = 1$ to $Z = 54$ over an angular range of $\theta = 2^\circ - 176^\circ$ (90% of 4π); very large dynamic in energy; detecting and identifying protons of 1-200MeV, and Uranium ions upto 4GeV; low energy particle identification

thresholds of between 0.7MeV/u and $\sim 1.3\text{MeV/u}$ ($Z = 3$ and $Z = 50$ respectively). Neutrons are not detected. In the aim of studying the single-source multifragmentation events contained in this experimental data we have considered the most commonly used methods of selecting single-source events based on global variables, and found that they can be arranged into three classes : (1) Impact parameter selectors (IPS); (2) Global shape variables (GSV); (3) Wilczyński diagram¹.

| V_∞ (cm/ns) | V_0 (cm/ns) | $\epsilon^*(Gd)$ (MeV/u) | $\epsilon^*(U)$ (MeV/u) |
|--------------------|---------------|--------------------------|-------------------------|
| $V_{beam} = 8.14$ | 7.34 | - | - |
| 6.95 | 6.00 | 3.30 | 2.10 |
| 5.32 | 4.00 | 6.40 | 4.20 |
| 4.04 | 2.00 | 8.30 | 5.40 |
| 3.65 | 1.00 | 8.75 | 5.70 |
| 3.51 | 0.00 | 8.90 | 5.80 |

Table 1: Parameters of the dissipative binary collisions simulations. Relative velocities of $QP(=Gd)$ and $QT(=U)$ are given at contact (V_0) and 'at infinity' (simple Coulomb calculation, V_∞), along with excitation energies for each source which correspond to equilibration of E^* . The relative velocities corresponding to the beam velocity are given for comparison, while $V_0 = 0.00$ ($V_\infty = 3.51$) corresponds to full damping.

The response of the latter two to the multifragmentation of a single source or of two sources with varying degrees of relaxation has been studied using the event generator SIMON[13]. In accordance with experimental results for the single source in Gd+U collisions (see [4][5][14]) the total mass ($A = 393$) and excitation energy ($\epsilon = 7.1\text{MeV/u}$) of the system are arranged in a 'freeze-out' configuration of 6 pre-fragments with a spherical geometry, with a self-similar radial expansion of 1MeV/u . For the 'binary collisions' simulations, the two outgoing excited partners were Gd+U in contact with initial relative velocity (V_0) making an angle of 10° with the beam direction, each source comprising 3 primary excited fragments placed in a spherical configuration (except for the least relaxed case for which, in accordance with the experimental results, it is more realistic to consider 3 initial fragments in total : a quasi-Gadolinium, and the two fission fragments of Uranium). For each value of V_0 /relaxation (see Table 1), the total excitation energy of quasi-projectile and quasi-target ($QP + QT$) was calculated simply using

$$E^* = E_{cm} - E_C - \frac{1}{2}\mu V_0^2, \quad E_C = \frac{Z_1 Z_2 e^2}{d}, \quad \mu = \frac{A_1 A_2}{A_1 + A_2} \cdot u \quad (1)$$

where d , the centre-centre distance between QP and QT, is equal to the sum of their radii calculated from the liquid-drop formula $r = r_0 A^{1/3}$, $r_0 = 1.22\text{fm}$; E_{cm} is the available centre-of-mass energy; and A_1, Z_1 etc. are the mass and charge numbers of QP and QT. E^* was shared equally between the two sources.

All events generated by SIMON were passed through an experimental filter, reproducing the geometrical and dynamical acceptance of the INDRA detector, in order to allow direct comparison of experimental and simulated data. As all methods considered use global variables it is essential to apply them only to events for which a maximum of information has been obtained. A 'standard' pre-selection has been applied to both experimental and simulated events to ensure well measured 'complete' events. This pre-selection takes the following form :

$$\frac{\sum Z}{Z_{total}} \geq 80\%, \quad \frac{|\sum Z \vec{v}|}{Z_p v_p} \geq 80\% \quad (2)$$

where the momentum is calculated as the product of particle charge and velocity, to neglect the effect of (unmeasured) neutrons. In addition to this control on the magnitude of the momentum, a further constraint was placed on the angle ψ made by the vector $\sum Z \vec{v}$ with the beam, restricting it to values $\psi < 6^\circ$.

2 Recognition and selection of single-source events using global variables

2.1 Impact parameter selectors (IPS)

Single-source events must be among the most central collisions and so one may reasonably hope to isolate the former by effecting a selection corresponding to retaining only the smallest impact parameters. As direct measurement of the impact parameter b is impossible some variable or variables must be found for which a good correlation with b is shown (by simulating the collisions). What we call impact parameter selectors (IPS) are 'simple' global variables to which this property is commonly attributed. IPS frequently encountered in the literature which we have considered in this study are

- N_C , total charged particle multiplicity
- N_{qp} , light charged particle (LCP : $Z = 1, 2$) multiplicity
- E_T , the total transverse energy (w.r.t. the beam direction)
- E_{T12} , the total transverse energy of LCP

all of which, it is generally accepted, increase with decreasing impact parameter.

The method of selecting single-source events then consists of retaining events having the highest values of N_C , E_{T1} , etc., corresponding to the most central collisions, assuming that these most central collisions lead to the formation and multifragmentation of a single source, to the exclusion of all other reaction mechanisms.

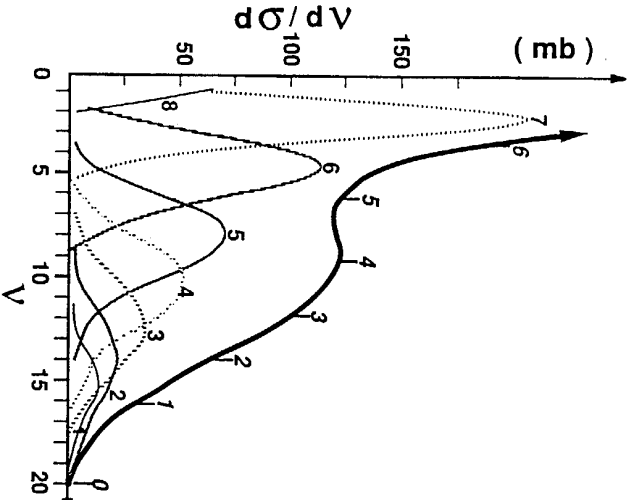


Figure 1: Total multiplicity (ν) distributions resulting from a simulation of collisions of $^{40}\text{Ar}+^{37}\text{Al}$ 45 MeV/u carried out in [16]. Individual distributions for 1 fm bins in the impact parameter b of the simulated collisions are shown, the number on each corresponding to the maximum b of the bin. The thick curve is the impact parameter-integrated distribution, corresponding to that which would be measured experimentally. Italic figures on this curve give the impact parameter scale b_{calc} calculated using the geometrical prescription (see text).

The first problem to mention in connection with this method in our opinion is the lack of "sharp cut-off" in impact parameter between binary and unary collisions. This means that it is not possible to use IPS to select all single-source events without

binary pollution. This is not fatal to the method; we may still select a reasonably uncontaminated sample of single-source events with reduced statistics, provided that the IPS chosen can permit us to select only events having impact parameters smaller than those for which binary collisions dominate. The geometrical prescription [15] permits the establishment of an impact parameter scale using IPS, as is shown in Fig. 1 for the example of simulated collisions of the system $\text{Ar}+^{37}\text{Al}$ 45 MeV/u, using as IPS the total multiplicity, N_C (ν in Fig. 1) [16].

$$b_{calc} = \frac{b_{max}}{\sqrt{N_{tot}}} \left[\int_{x(b)}^{x_{max}(b=0)} \frac{dN}{dx} dx \right]^{\frac{1}{2}} \quad (3)$$

where $\frac{dN}{dx}$ is the number of events having a value of the IPS x between x and $x + dx$, N_{tot} is the total number of measured events, and b_{max} is the maximum impact parameter of the collisions.

First of all it can be seen in Fig. 1 that the distributions of ν/N_C for each 1 fm bin in b are wide and overlap each other significantly. Because of this the calculated impact parameter binning b_{calc} is approximative and mixes collisions with different b . This mixing increases as collisions become more central. Secondly, although for the largest values of b the binning is acceptably approximative, the complete overlap between multiplicity distributions for the most central simulated collisions ($0 < b \leq 1 \text{ fm}$, $1 < b \leq 2 \text{ fm}$) renders the method incapable, in this example, of distinguishing between impact parameters $b < 2 \text{ fm}$ (in practice this lower limit could be increased by the need to retain a sample with workable statistics, thus relaxing the severity of the ν/N_C 'cut'). The existence of a finite limit on the centrality of the collisions selected implies the impossibility of isolating a sample of single-source events with negligible binary pollution in this way if binary reactions are the dominant mechanism at and below the limiting impact parameter ($\leq 2 \text{ fm}$ in the example shown).

In conclusion

- (i) the assumptions underlying the selection approach i.e. the correlation between IPS and b depends on some model(s) of the collisions
- (ii) an impact parameter selection cannot give all single-source events with no binary pollution, due to the absence of "sharp cut-off"
- (iii) the 'most central' collisions that can be isolated may be irretrievably polluted by binary reactions, due to large fluctuations of IPS for the most central collisions

For these three reasons we believe that methods based on impact parameter are not the best way to approach the problem of single-source selection.

It should be remembered, however, that as can be seen in Fig. 1, IPS do provide a very acceptable and effective method of classifying events according to impact parameter, from peripheral to central collisions with the double proviso that the calculated impact parameter becomes more and more approximative with increasing centrality, and that there is no reason *a priori* to expect the ‘most central’ collisions selected to correspond to a highly pure sample of single-source events. Depending on the experimental apparatus at one’s disposal, it is not always possible to effect more elaborate selections based on, for example, global analyses of the fragment momenta and energy in each event. This is the second method considered, to which we now turn our attention.

2.2 Global shape variables (GSV)

A single multifragmenting source, in thermal equilibrium and having little or no spin, will emit particles and fragments isotropically (in its rest frame). On the other hand, multifragmentation of the two separating sources of a binary reaction will produce emission patterns that are elongated in the sense of their relative velocity. We can measure the form of the resulting distributions of energy/momentum of the emitted particles, and try in this way to distinguish single-source from binary events. Examples of global shape variables (GSV) used for this purpose are presented in Table 2 : they are the second moment of Fox and Wolfram, $H(2)$ [17], the momentum isotropy ratio R_{iso} [18], and the energy isotropy ratio E_{iso} .

| GSV | single source | binary reactions |
|--|---------------|------------------|
| $H(2) = \frac{\sum_{\nu,\rho} (1/2) \vec{p}(\nu) \vec{p}(\rho) (3 \cos^2 \theta_{\nu\rho} - 1)}{\sum_{\nu,\rho} \vec{p}(\nu) \vec{p}(\rho) }$ | 0 | 1 |
| $R_{iso} = (2/\pi) \sum_{\nu} \vec{p}_\perp(\nu) / \sum_{\nu} \vec{p}_\parallel(\nu) $ | 1 | 0 |
| $E_{iso} = 1 - \frac{(3/2) \sum_{\nu} \vec{p}_\perp^2(\nu) / 2m(\nu)}{\sum_{\nu} E(\nu)}$ | 0 | 1 |

Table 2: Definitions of GSV considered in Sec. 2.2, and their infinite-multiplicity responses to isotropic (single-source) and ‘two jet’ (binary) emission. All sums are over fragments ($Z \geq 5$) in the centre of mass of reaction (see text).

As light charged particles do not have a unique origin in the reactions (secondary

emission, ‘prompt’ emission), these variables are calculated using only the momenta or energy of the fragments in each event, defined as detected nuclei having $Z \geq 5$. As our intention is to seek events in which nearly all 393 nucleons participate in the formation of a single source, we suppose that the recoil velocity of the latter will not deviate appreciably from the velocity of the centre of mass of the reaction, and that recoil velocity fluctuations due to the ‘fusion’ being more or less incomplete are less significant than the systematic error on the measured velocity of the fragments’ centre of mass due to incomplete detection and secondary emission. The GSV are therefore calculated in the centre of mass of reaction frame.

$H(2)$ depends on relative angles between fragment momenta and on their absolute magnitudes, and is therefore invariant under a rotation of the coordinate axes. The two isotropy ratios, defined in terms of projections of energy or momenta perpendicular and parallel to a given axis, are clearly rotation-dependent. A natural choice for the ‘reference’ axis would appear to be the velocity of the fragments’ centre-of-mass frame (assumed here to be the beam direction); however the values of E_{iso} and R_{iso} would then vary as a function of the scattering angle of the two outgoing partners of deeply inelastic collisions, giving different responses for the same degree of relaxation (i.e. same event form), and indeed for any given form of the energy/momentum distributions one can always find an orientation with respect to the beam axis such that E_{iso} and R_{iso} give their ‘single-source’/isotropic values (or any other values). This ambiguity in the response obviously has to be lifted in order to be able to effect a selection of isotropic-form events corresponding to the fragmentation of a single source. If the scattering angle were constant, e.g. if the two partners’ relative velocity were always aligned with the beam (reference) axis, the problem would not exist. The solution is therefore to find the direction of the relative velocity of the two partners, and then to calculate E_{iso} and R_{iso} with respect to this axis, referred to as ‘direction of maximum fragment KE flow’ in the figures (see Sec. 2.3 below).

The most important characteristic and handicap of GSV-based approaches is their sensitivity to small number effects[19][20]. In general their response depends on the multiplicity (of fragments in our case) of the event, getting worse (i.e. deviation of $<GSV>$ from ‘true’ value and σ_{GSV} increase) as the multiplicity decreases.

In Fig. 2 is shown the response of E_{iso} to simulated single-source events for different multiplicities of fragments N_f . It can be seen that in all cases the distributions of the GSV are very wide due to the small number of fragments ($5 \leq N_f \leq 8$), corresponding to a large range of different event shapes, while the mean values are far from that

Gd+U 36MeV/u - SIMON+INDRA filter - Single Source

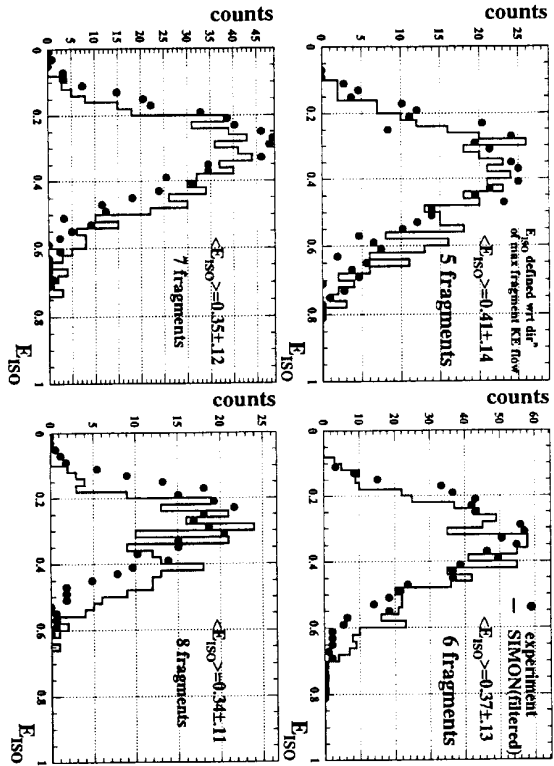


Figure 2: Histograms : response of the GSV E_{iso} to the simulated multifragmentation of a single source. Points : experimental data selected using the Wilczyński method. Events with different fragment multiplicities are treated separately. E_{iso} is unambiguous, i.e. calculated with respect to the direction of maximum fragment KE flow derived from the momentum tensor (see Sec.2.2 and Sec.2.3). The mean values and standard deviations given are for the simulated distributions.

corresponding to an isotropic distribution of fragment kinetic energies, $E_{iso} = 0$ ($< E_{iso} > \approx 0.3 - 0.4$). The response is seen to improve as N_f increases.

The problem is not the following : the distributions of fragment kinetic energies (or momenta) are isotropic but the GSV are incapable of measuring them correctly. In order that the final distributions of fragments emitted isotropically correctly represent the form of the emission law, the particles must be infinite in number: the smaller their number, the greater the discontinuous "lumpy" nature of the resulting distributions which is inconsistent with high isotropy. The problem, therefore, is that the isotropic emission of a finite number of particles leads to energy/momentum distributions which are not isotropic, and whose forms are subject to large fluctuations.

It is shown in Fig.3 that for the fragmentation of a single source, the distribution of $\cos \theta$ of fragments (accumulated over many events) is flat (therefore they are emitted

Gd+U 36MeV/u - SIMON+INDRA filter - Single Source

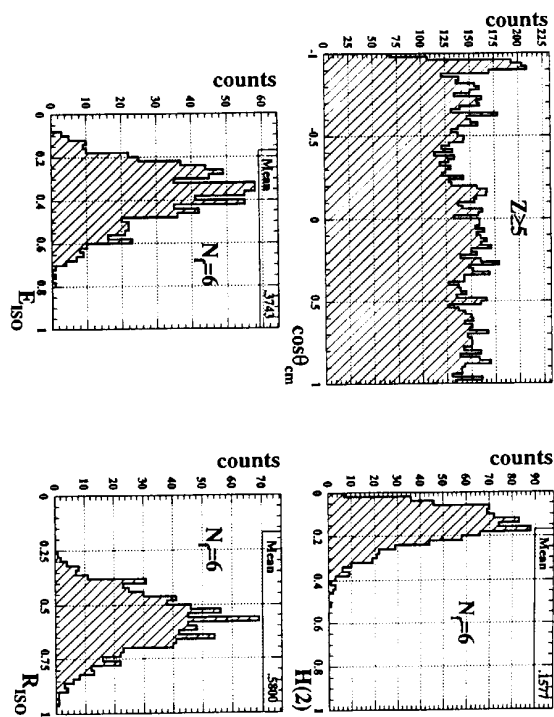


Figure 3: (upper left) Simulated angular distribution of fragments in the centre of mass frame for single-source events. (clockwise from top right) Simulated distributions of GSV $H(2)$, R_{iso} , and E_{iso} for these events. The multiplicity of fragments is 6 in each case.

isotropically) while the distribution of, say, R_{iso} for a given N_f (value calculated event by event) is centred far from 1 ($N = \infty$ isotropy response) and very wide¹. The distribution of $\cos \theta$ represents correctly the isotropic nature of the emission law – it is accumulated over a large number of events, and so corresponds effectively to a multiplicity $N_f \rightarrow \infty$. Event by event we measure only $N_f \rightarrow 0$ values of $\cos \theta$, from which it is very difficult to infer the form of the underlying emission law : this is exactly what the GSV try to do.

¹It is interesting to note that for the same finite N_f , both R_{iso} and E_{iso} , when calculated with respect to the beam axis give distributions for isotropic/single-source emission which are centred around their respective infinite multiplicity responses. They cannot be used to select single-source events due to the ambiguous response problem mentioned above, but they may be used to gauge whether a sample of events corresponds to single-source events or not, as the probability of a sample of binary events having just the right orientations with the beam axis to give a distribution centred around the theoretical single-source response seems quite low. However attention must be paid to any correlations between the selection method and these variables (cf. $\theta_{flow} - E_{iso}/R_{iso}$, see Sec.2.3)

If perfect isotropic emission requires $N_f = \infty$ for correct GSV response, the extreme case of a binary reaction with a very large relative velocity ($V \rightarrow c$) between the

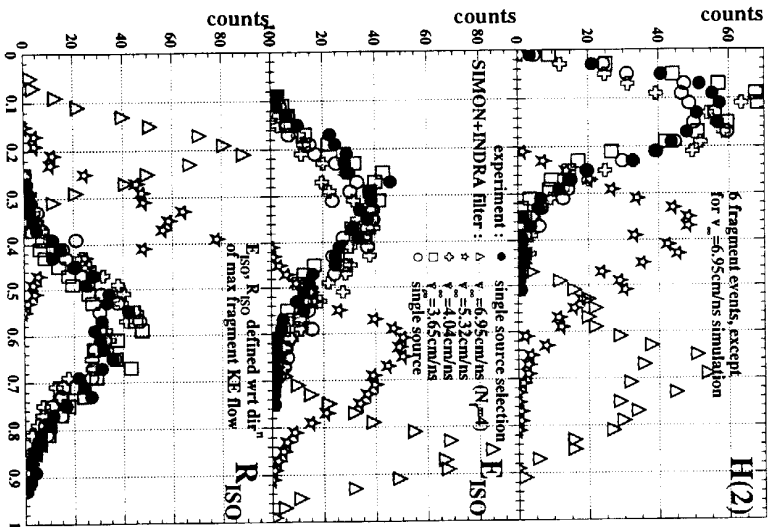


Figure 4: Simulated response of the three GSV considered to increasingly relaxed binary collisions, and to a single-source decay (open symbols), showing that the response to highly relaxed binary reactions is indistinguishable from the fragmentation of a single-source. Solid points : experimental data selected using the Wilczyński method.

two sources, giving a linear, 2-jet form to the final state fragment distributions, implies that only 2 fragments are theoretically necessary to exactly reproduce the emission law (a line). As the relative velocity decreases (increasingly dissipative/relaxed collisions) its role as determining factor in the form of the final state distributions becomes less important compared to that of mutual Coulomb interactions between fragments issued

from different sources, which tend to increase the isotropy of the distributions. Therefore for a given N_f ($2 < N_f < \infty$) the response of GSV worsens as we pass from binary collisions with low relaxation to highly dissipative binary reactions, and finally becomes worst of all for single-source events (as the emission of fragments becomes increasingly isotropic).

Finally, the separation of binary and single-source events by GSV selection supposes sufficiently different GSV responses in the two cases. Fig.4 shows that this is not so for highly-relaxed binary collisions, corresponding to $V_\infty \leq 4.04 \text{ cm/ns}$ (cf. Table 1), for which the response of GSV saturates and is indistinguishable from the response to a single-source decay. High isotropy of the energy/momentum etc. distributions measured in this way is therefore no guarantee of a disappearance of binary character from the reactions.

In conclusion,

- GSV selection is not model-dependent; however it is based on the assumption of a thermalised, low-spin source
- GSV analysis is multiplicity dependent, and apart from the effects detailed above, this means that there in fact should be different selection criteria for different fragment multiplicities. However, this point is normally neglected as the selection ($H(2) < 0.1$, $R_{iso} > .9$ etc.) is a rather arbitrary balancing of the desire to keep only the most isotropic events with the need for a sample with workable statistics.
- the idea behind GSV selection is that one source or two sources do not give the same emission law, but we cannot measure this law, only the resulting distributions of a small finite number of particles :
 - (i) energy/momentum distributions of a finite number of particles emitted isotropically are *anisotropic*, and subject to large fluctuations
 - (ii) the distributions of highly damped binary reactions and those of single-source events are indistinguishable

2.3 The 'Wilczyński diagram' technique

The third and final method we discuss is based on two other characteristics of single-source events : the formation of a single-source corresponds to collisions in which a

maximum of energy is dissipated, and no preferred direction of the global ‘flow’ of the final fragment kinetic energies exists (corresponding to a loss of memory of the entrance channel, *i.e.* assuming thermalisation of the source and negligible angular momentum effects). This method, the ‘Wilczyński diagram’ technique introduced by J.F. Lecoilley and co-workers for the system Pb+Au 29MeV/u[1], which exploits two characteristics of single-source events, is therefore a crossed method using two different global variables.

The first variable is the total measured kinetic energy TKE, defined as the sum of centre of mass kinetic energies of all detected reaction products, which can also be expressed as

$$\text{TKE} = E_{CM} + Q - \sum E_{\text{neutron}} \quad (4)$$

As collisions become more and more dissipative, more of the relative kinetic energy of target and projectile is converted to excitation energy. The greater the excitation energy, the greater the average number of unmeasured neutrons (and the higher their average energy) and fragments with $Z \geq 5$ (which reduce Q , *i.e.* make it more negative) in the exit channel of the reaction. Therefore TKE decreases with increasing dissipation.

In order to establish a ‘preferred direction’, if one exists, the tensor of [21] is constructed from the components of fragment centre of mass momenta,

$$Q_{ij} \equiv \sum_{Z \geq 5} \omega_i p_i p_j \quad (5)$$

with $\omega = \frac{1}{2m}$, giving the tensor of fragment kinetic energy flow in each event. The eigenvectors and eigenvalues of Q_{ij} define an ellipsoid in energy space which represents the event form in exactly the same way as the GSV described in Sec.2.2 above, and all the same comments apply here. The ‘sphericity’ S [21], commonly used to describe the event shape derived from the eigenvalues of Q_{ij} , was not treated as a case apart in Sec.2.2 as, unsurprisingly, there exists a simple relationship between this variable and the GSV E_{iso} when the latter is calculated unambiguously (*i.e.* with respect to the ellipsoid major axis) (see below and Sec.2.2) :

$$S = 1 - E_{iso} \quad (6)$$

The direction of the major axis of the ellipsoid, *i.e.* the eigenvector corresponding to the largest eigenvalue of Q_{ij} , is referred to by its polar angle with respect to the beam, θ_{flow} . This is the direction which maximises the global flow of fragment kinetic energy, and is the ‘preferred direction’ for each event referred to above.

As stated in Sec.2.2 the event forms for fragments issued from binary reactions are prolate ellipsoids whose major axis is aligned with the relative velocity of the two

Gd+U 36MeV/u - SIMON+INDRA filter: Binary/Single-source

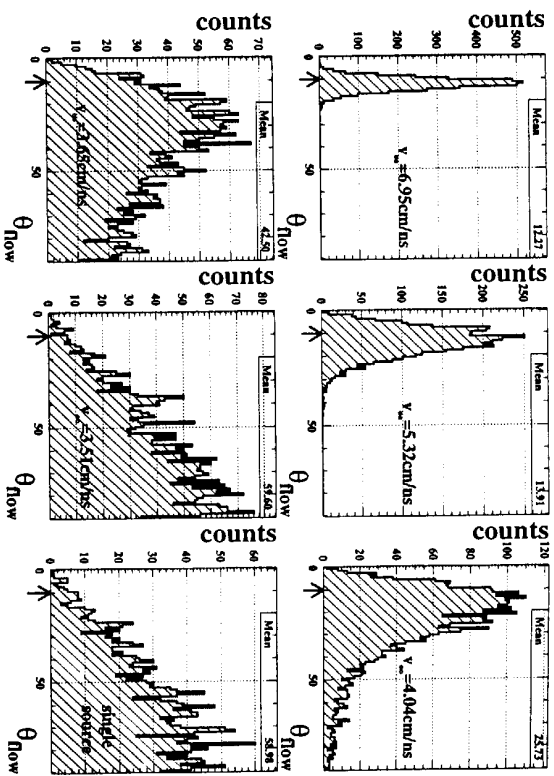


Figure 5: Distributions of θ_{flow} obtained for simulated binary collisions with different degrees of relaxation, and for the simulation of a single source. The arrows below the abscissa indicate the position of $\theta_{cm} = 10^\circ$.

sources. Therefore for binary collisions

$$< \theta_{flow} > \simeq \theta_{cm} \quad (7)$$

where θ_{cm} is the centre of mass scattering angle of QP and QT². In Fig.5 are shown the distributions and mean values of θ_{flow} obtained for all simulations described in Sec.1. It should be remembered that for each two-source simulation, the initial relative velocity of QP and QT is inclined at an angle of 10° with respect to the beam axis, corresponding to a constant scattering angle θ_{cm} . It can be seen that Eq.7 holds for the least dissipative cases ($V_\infty > 4.04 \text{ cm/ns}$), but as the relaxation becomes more complete (*i.e.* as the distribution of fragment kinetic energy becomes more isotropic) the distribution of θ_{flow} becomes wider and wider, and at full relaxation ($V_\infty = 3.51 \text{ cm/ns}$) it is indistinguishable from that produced by the single-source events. Note that for $V_\infty = 4.04 \text{ cm/ns}$ although

²This is why E_{iso} and R_{iso} are calculated with respect to the major axis of the ellipsoid (direction of maximum fragment KE flow in Fig.2 and Fig.4) in order to remove the ambiguity highlighted in Sec.2.2

the distribution is rather large, only a very small proportion ($\sim 12\%$) of events explore values of $\theta_{flow} > 45^\circ$, for this same relaxation the GSV response is indistinguishable from single-source emission (cf. Fig. 4). Even for more complete relaxation ($V_\infty = 3.65 \text{ cm/ns}$) although the proportion of events with $45^\circ < \theta_{flow} \leq 90^\circ$ is significant ($\sim 42\%$), the distribution is still clearly peaked at more forward angles ($< \theta_{flow} > = 42.5^\circ$).

In Sec. 2.2 it was seen that the energy/momentum distributions event by event for the break up of a single source are not isotropic due to the finite (small) fragment multiplicity, which is the primary handicap of GSV selection methods. This residual anisotropy of the distributions means that a direction of maximum energy flow, θ_{flow} , can still be found even for single-source events, but as it is due to small number effects and not to some memory of the entrance channel, it is randomly directed even though the distributions are not isotropic i.e. the ellipsoid is not a sphere. This approach actually uses the weakness of GSV to its advantage. The multifragmentation of a single source is therefore associated with a flat distribution

$$\frac{d\sigma}{d(\cos \theta_{flow})} = \text{constant} \quad (8)$$

or distributions of θ_{flow} which are proportional to $\sin \theta_{flow}$ and single-source events are concentrated at large flow angles. 73% of them having $\theta_{flow} > 45^\circ$ (54% have $\theta_{flow} \geq 60^\circ$) (see Fig. 5). Importantly, Eq. 7 and Eq. 8 are independent of the fragment multiplicity.

The distribution of $\cos \theta_{flow}$ is a good indicator of whether or not single-source events are present in a given sample and to what degree they are mixed with binary collisions. If the events do not explore all values of $\cos \theta_{flow}$ it is certain that none of them correspond to the deexcitation of a single source. If the distribution is peaked and all values are explored, single-source events may be present, with the dominance of binary reactions depending on the ratio of the area under the peak to the total area of the distribution. If above a certain value of θ_{flow} the distribution becomes flat, the corresponding events are good candidates for single-source multifragmentation with negligible pollution from binary reactions.

We may apply this method of discrimination to samples of Gd+U collisions selected using the approaches described in Sec. 2.1 and Sec. 2.2. Fig. 6 and Fig. 7 show, for the IPS N_C and the GSV $H(2)$ respectively, $\cos \theta_{flow}$ distributions obtained for three increasingly stringent cuts using each variable. In both cases it can be seen that for all 'cuts', which go right to the limits of acceptable statistics for the selected events, the resulting distributions remain stubbornly anisotropic, with a strong peak around the beam direction ($\theta_{flow} = 0$) and long tails which are almost flat for $\theta_{flow} > 60^\circ$

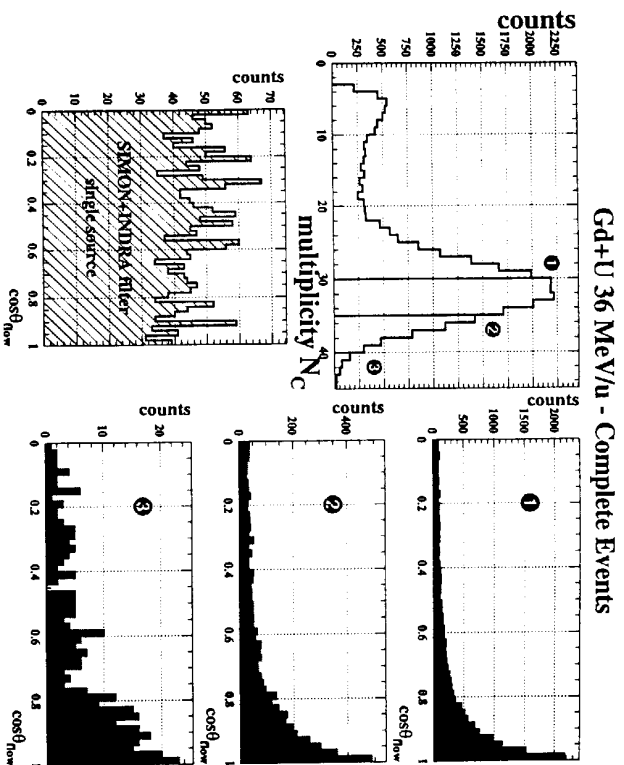


Figure 6: (upper left) Distribution of N_C for complete events, Gd+U 36 MeV/u, indicating three 'cuts' for most central collisions : 1 $N_C > 30$; 2 $N_C > 35$; 3 $N_C > 40$. (bottom left) Distribution of $\cos \theta_{flow}$ for the simulated single-source events. (right) Distributions of $\cos \theta_{flow}$ obtained by applying the three N_C 'cuts'.

($\cos \theta_{flow} < 0.5$). Upon examining the events in the peak and in the tail the former are found to be dominantly binary in nature, while for the latter no binary character can be perceived[4][14].

Therefore in accordance with Sec. 2.1 and Sec. 2.2 single-source events for collisions of Gd+U at 36 MeV/u selected using IPS and GSV have a large pollution by binary reactions no matter how swinging the conditions applied to them. By effecting a subsequent sorting of events depending on θ_{flow} we can apparently remove that part of the sample which is dominated by binary collisions. But then the initial selection by IPS or GSV is redundant, and can be abandoned.

The 'Wilczyński diagram' technique uses the discriminatory power of the $\cos \theta_{flow}$ distribution to isolate single-source events for the most dissipative collisions selected with TKE. Its name comes from the fact that plots of TKE vs. θ_{flow} [10][1] such as

Gd+U 36 MeV/u - Complete Events

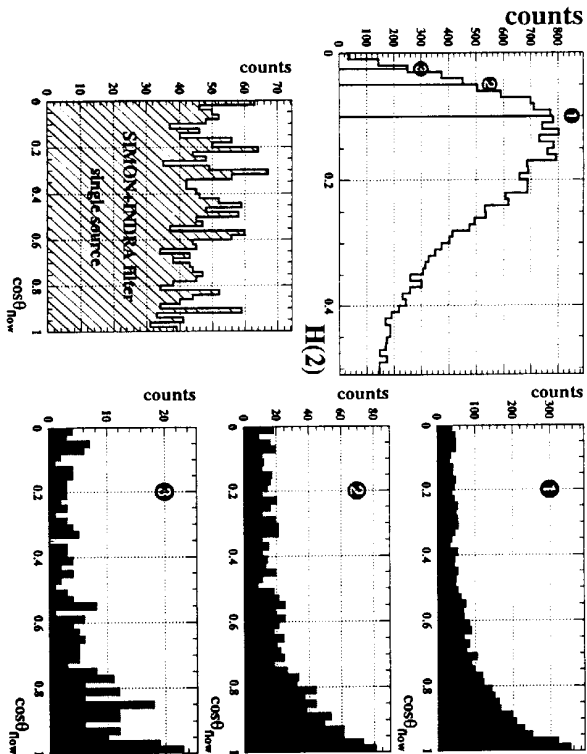


Figure 7: (upper left) Distribution of $H(2)$ for complete events, $Gd+U$ 36MeV/u, indicating three 'cuts' for most isotropic event forms: 1 $H(2) < 0.1$; 2 $H(2) < 0.05$; 3 $H(2) < 0.025$. (bottom left) Distribution of $\cos\theta_{flow}$ for the simulated single-source events. (right) Distributions of $\cos\theta_{flow}$ obtained by applying the three $H(2)$ 'cuts'.

that shown in Fig.8 bear a strong resemblance to those of the double differential cross-section $d^2\sigma/dE d\Omega_{cm}$ used at lower energies. J. Wilczynski successfully interpreted the forms of these plots, of centre-of-mass energy versus scattering angle for one of the two partners of a deeply inelastic collision, in terms of dissipative nuclear orbiting[22][10].

θ_{flow} is analogous to the scattering angle for binary collisions that are not too relaxed (Eq.7), i.e. for events with $TKE > 2156\text{MeV}$ (see Fig.8), and therefore related to the degree of orbiting of the system. It can be seen in the diagram that below 2156MeV the distribution of θ_{flow} is very large, exploring all values. However it has been shown that for a fixed value of Ω_{cm} with large degrees of dissipation, a very large range of θ_{flow} is explored (Fig.5), thus any connection with the rotation of the system $QP+QT$ is lost. The distribution of $\cos\theta_{flow}$ for these most dissipative events is strongly peaked in the beam direction, corresponding to the dominant binary reactions as we saw above, and

Gd+U 36MeV/nucleon - Complete events

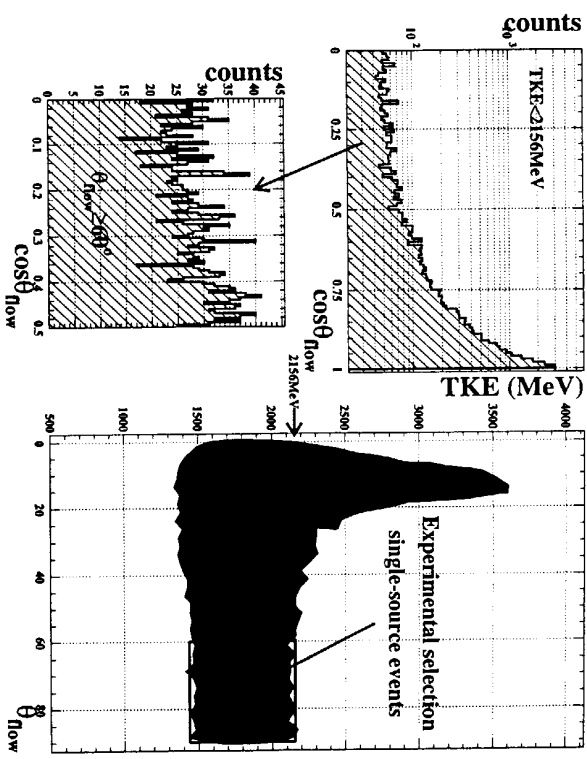


Figure 8: (upper left) Distribution of $\cos\theta_{flow}$ for the most dissipative collisions of $Gd+U$ ($TKE < 2156\text{MeV}$). (lower left) As above, but only for $\theta_{flow} \geq 60^\circ$ and with a linear ordinate scale. (right) 'Wilczynski diagram', TKE vs. θ_{flow} for complete events, $Gd+U$ 36MeV/u. The box corresponds to the selection of single-source events.

flattens out for $\theta_{flow} \geq 60^\circ$, suggesting a negligible contribution from anything other than single-source events at these large angles. These are the events selected and analysed in terms of the multifragmentation of a single source comprising the near-totality of available excitation energy and nucleons in [4][5][14]. The selected events correspond to a cross-section of 22mb , and as we found 54% of simulated events to have $\theta_{flow} \geq 60^\circ$, an upper estimate (assuming zero pollution of the sample) of the total cross-section for single-source events is 41mb , to be compared with a total reaction cross-section $\sigma_R \sim 60[23]$.

3 Conclusions and Outlook

In this contribution we have studied in detail some commonly-used methods of selecting single-source events in heavy ion collisions at GANIL energies, and tested them with simulations and experimental data for collisions of $\text{Gd}+\text{U}$ 36MeV/u measured with INDRA. We have insisted on the fact that impact parameter selectors (e.g. total multiplicity, transverse energy) and global shape variables (e.g. Fox moments) may be incapable of selecting single-source events without large contamination by the binary processes which dominate the reaction cross-section at these energies. This has been shown to be the case for $\text{Gd}+\text{U}$, while for an almost identical system ($\text{Au}+\text{Au}$ 35MeV/u [24]) the same technique (analysis of the form of the selected events' $\cos\theta_{\text{low}}$ distribution) seems to demonstrate the contrary.

The 'Wilczyński diagram' technique introduced in [1] has been shown to be the only one considered in this contribution which permits the selection of a sample of single-source events with good statistics ($\sim 50\%$ of single-source events selected with $\theta_{\text{low}} \geq 60^\circ$) and negligible pollution by binary reactions. These events are analysed and discussed in detail in terms of what they can tell us about the multifragmentation process in very heavy systems in [5], [4], and [14].

The selection used is model-independent, multiplicity-independent, and is 'neutral' in the sense that what we select are good candidates for unpolluted single-source events, but their character has to be verified by detailed analysis. However, the method, as presented here, is within the rather narrow framework of a source in thermal equilibrium and having no angular momentum.

While the assumption of the thermalisation of incident energy in the source so that final fragment kinetic energies and momenta are randomised would appear to be inevitable for any approach based on event forms, isotropy, etc., the question of the maximum spin of any source that one might select is an important one[25]. In addition, we have argued in this contribution in terms of an opposition of single-source events and binary collisions, while it has been shown experimentally[26][27] that a significant proportion of particles and intermediate mass fragments emitted in mid-peripheral to central collisions come from a mid-rapidity 'neck'-like source formed between QP and QT. Work is in progress to extend the scope of this study to include both of these aspects of heavy-ion collisions at 20-100MeV/u as they are experimentally understood today.

References

- [1] J.F. Lecolley et al., *Physics Letters B* 387(1996)460-465
- [2] N. Marie et al., *Physics Letters B* 391(1997)15
- [3] R. Bougault et al., this conference
- [4] Ch.O. Bacci et al., *Proc. XXXIV Int. Winter Meeting on Nuclear Physics*, Bormio (Italy) 1996 ed. I. Iori, Ricerca scientifica ed educazione permanente, page 46.
- [5] M.F. Rivet et al., this conference
- [6] P. Bonche et al., *Nuclear Physics A* 436(1985)265
- [7] B. Borderie et al., *Physics Letters B* 302(1993)15
- [8] B. Borderie et al., *Physics Letters B* 205(1988)26; M.F. Rivet et al., *Proc. XXXI Intern. Winter Meeting on Nuclear Physics*, Bormio, (Italy) 1993, ed. I. Iori, Ricerca scientifica ed educazione permanente, page 92.
- [9] R. Bougault et al., *Nuclear Physics A* 587(1995)499-512
- [10] J.F. Lecolley et al., *Physics Letters B* 325(1994)317
- [11] J. Péter et al., *Nuclear Physics A* 593(1995)95-123
- [12] J. Pouthas et al., *Nuclear Instruments and Methods A* 357(1995)418
- [13] D. Durand, code SIMON, in preparation
- [14] M. Squalli, *Ph.D Thesis*, Université de Paris XI 1996
- [15] C. Cavata et al., *Physical Review C* 42(1990)1760
- [16] J. Péter et al., *Nuclear Physics A* 519(1990)611
- [17] G.C. Fox and S. Wolfram, *Physics Letters B* 82B(1979)134 and *ibid. Nuclear Physics B* 149(1979)413—496
- [18] A. Kerambrun, LPCC 93-02(1993)
- [19] P. Danielewicz and M. Gyulassy, *Physics Letters B* 129B(1983)283.
- [20] V. Métivier, *Ph.D Thesis*, Université de Caen 1995
- [21] J. Cugnon and D. L'Hôte *Nuclear Physics A* 397(1983)519
- [22] J. Wilczyński, *Physics Letters B* 47B(1973)484
- [23] W.W. Wilcke et al., *At. Dat. and Nuc. Dat. Table* 25(1980)391
- [24] M. D'Agostino et al., *Physics Letters B* 368(1996)259
- [25] M. D'Agostino et al., this conference
- [26] J.F. Lecolley et al., *Physics Letters B* 354(1995)202-207
- [27] J. Lukasiak et al., *Physical Review C*, in press